Soil Biology and Biochemistry 162 (2021) 108420

Contents lists available at ScienceDirect

Soil Biology and Biochemistry

journal homepage: www.elsevier.com/locate/soilbio

Bacterial community structure and putative nitrogen-cycling functional traits along a charosphere gradient under waterlogged conditions

Mengjie Yu [a,b], Wei-qin Su [a,b], Laibin Huang [c], Sanjai J. Parikh [c], Caixian Tang [d], Randy A. Dahlgren [c], Jianming Xu [a,b,*]

[a] Institute of Soil and Water Resources and Environmental Science, College of Environmental and Resource Sciences, Zhejiang University, Hangzhou, 310058, China
[b] Zhejiang Provincial Key Laboratory of Agricultural Resources and Environment, Hangzhou, 310058, China
[c] Department of Land, Air and Water Resources, University of California, Davis, CA, 95616, USA
[d] Department of Animal, Plant & Soil Sciences, Centre for AgriBioscience, La Trobe University, Bundoora, VIC, 3086, Australia

ARTICLE INFO

Keywords:
Biochar
Bacterial community structure
Nitrification
Denitrification
N_2-fixation
N transformations

ABSTRACT

Unique spatial niches created by biochar form a dynamic biogeochemical soil zone, termed the "charosphere". Charosphere soil has different properties from either soil or biochar, often acting as a hotspot for microbial activity. However, the direction and magnitude of charosphere effects on soil processes and microbial communities remain inconclusive. Herein, we designed a multi-sectional box to separate charosphere soils from biochar under waterlogged conditions, investigating millimeter-scale changes in bacterial communities and distributions of specific genera across the charosphere created by pristine biochar (produced from corn stover at 300 °C), acid-modified biochar and washed biochar. The pristine biochar did not increase bacterial α-diversity but altered bacterial composition by promoting the growth of specific bacterial taxa and suppressing other species. In comparison, washed and acid-modified biochar increased the bacterial α-diversity. The pristine biochar significantly decreased N_2O emission and NO_3^- concentration owing to a lower soil nitrification potential. Abundances of N-cycling functional taxa were higher in the near-charosphere than outer-charosphere zone, especially for *Bacillus* (N_2-fixation), *MND1* (ammonia oxidation) and *Rhodopseudomonas* (denitrification). The spatial distribution of functional genes and genera documents the importance of heterogeneity within the charosphere gradient, providing a novel perspective into functional geometry to understand how biochar reduces N losses from agroecosystems.

1. Introduction

Anthropogenic nitrogen (N) loss from agricultural lands to aquatic ecosystems and the atmosphere creates severe environmental impacts, such as eutrophication and greenhouse effects induced by NO_3^- leaching and N_2O emissions, respectively (Liu et al., 2018; Zhu et al., 2014). Hence, there is an urgent need to develop sustainable agricultural strategies to attenuate N losses from soil systems (Molina-Herrera et al., 2016; Lam et al., 2017). Biochar, derived from biomass pyrolysis (300–700 °C) under oxygen-limited conditions, is considered a potential environment-friendly technology to regulate N-cycling processes in soil (Lehmann and Joseph, 2015; Pokharel et al., 2020). Biochar application to soil alters the physicochemical habitat for microbial communities, which influences microbially-regulated biogeochemical pathways (Gul and Whalen, 2016; Yu et al., 2021). Keystone microbial groups responsible for nitrification, denitrification, N_2-fixation and other N-cycling processes are considered as "ecosystem engineers", which are crucial in altering soil functions and subsequent agricultural productivity and environmental quality (Ma et al., 2021; Yue et al., 2019). Therefore, it is important to elucidate how biochar affects microbial community structure and functional traits related to N cycling (Dai et al., 2021; Zhang et al., 2018). However, few studies have focused on the bacterial community and functional effects, especially in terms of spatial variability across the biochar-soil interactive zone.

Novel spatial niches created by biochar form a dynamic biogeochemical zone coupling many interacting processes (Karppinen et al., 2019). This special soil zone surrounding a biochar source is termed the "charosphere" and may extend several millimeters into the adjacent soil

* Corresponding author. Institute of Soil and Water Resources and Environmental Science, College of Environmental and Resource Sciences, Zhejiang University, Hangzhou, 310058, China.
E-mail address: jmxu@zju.edu.cn (J. Xu).

https://doi.org/10.1016/j.soilbio.2021.108420
Received 12 January 2021; Received in revised form 24 August 2021; Accepted 6 September 2021
Available online 10 September 2021
0038-0717/

(Quilliam et al., 2013; Yu et al., 2019). It represents an ecotone gradient, with zones of transition between two different adjacent habitats (biochar and soil) (Gosz, 1993; Kolasa and Zalewski, 1995). Biochar directly influences the physicochemical properties of the charosphere, thereby affecting microbial dynamics and enzyme activities (Pei et al., 2017; Pingree and DeLuca, 2017). Luo et al. (2013) reported that biochar changed the charosphere soil environment to affect microbial habitats by altering pH, porosity and nutrient availability. However, it remains unclear specifically how, and to what extent, these changes altered microbial community composition and function, and how they propagate into the soil surrounding the biochar source and for how long these effects persist. Thus, a rigorous study of N metabolism in response to biochar along the ecotone with distinct differences in soil physicochemical properties and microbial community is necessary to disentangle N-cycling mechanisms across the charosphere.

Herein, we developed an experimental approach to examine millimeter-scale changes within the charosphere and used acid-modified and water-washed biochars to mimic an accelerated aging process, elucidating the effects of biochar on N-cycling processes and putative microbial functions across both spatial (increasing distance from biochar source) and temporal (biochar aging) scales. Specific objectives were to (1) assess the role of alkalinity and biochar derived solutes on bacterial community composition; (2) investigate variations of soil bacterial diversity and community structure due to changing physicochemical properties across the charosphere gradient; and (3) examine the distribution of N species and pertinent bacterial genera across the charosphere gradient. We hypothesized that if biochar was placed centrally in soil under waterlogged conditions to investigate spatial heterogeneity of the charosphere, the influences of biochar on soil N-cycling processes, such as mitigating the loss of N_2O and NO_3^-, would differ along the charosphere gradient. These changes are hypothesized to result from the spatial distribution of bacterial communities and specific species that alter N-cycling functional traits with distance across the charosphere.

2. Materials and methods

2.1. Soil and biochar characteristics

Soil (composite of 5 random sampling points) was collected from the upper 20-cm layer of an agricultural field with a rice-wheat rotation in Jinhua, Zhejiang Province, China (E119°64′, N28°98'). The soil was classified as an Acrisol (World Reference Base for Soil Resources). Plant residues were removed before the soil was air-dried and passed through a 2-mm sieve. Relevant soil characteristics were pH, 4.6 (1:2.5 H_2O, w/v); total C, 11.0 g kg^{-1}; total N: 0.9 g kg^{-1} and a sandy loam texture (636 g kg^{-1} sand; 196 g kg^{-1} silt; 168 g kg^{-1} clay).

Pristine biochar was produced from corn stover at 300 °C for 2 h in an oxygen-limited environment of a muffle furnace. After cooling, biochar was ground and sieved to isolate the 0.25–2 mm fraction, which was used in the study. Acid-modified biochar was prepared by impregnating the pristine biochar in Milli-Q water (1:10 w/v) with 1 M HCl until reaching a pH of 7. HCl was chosen rather than HNO_3 or H_2SO_4 because it better preserves biochar structure (Peterson and Brown, 2020). After 48 h, the mixture was oven-dried directly at 60 °C to a constant weight. To remove the dissolved substances from biochar, washed biochar was prepared by shaking the pristine biochar with Milli-Q water (1:10 w/v) at 120 rpm for 2 h before filtering and discarding the <25-μm leachate. The extraction process was repeated until the dissolved organic C concentration in the aqueous extract was <10 mg L^{-1}. The washed biochar was then oven-dried at 60 °C. Selected physicochemical properties of the biochar materials are provided in Table 1.

2.2. Incubation experiment

A multi-sectional box (length × width × height: 150 × 100 × 200 mm) (Fig. 1) was used to study the charosphere (modified from Yu et al., 2019). This design consisted of five distinct compartments: central biochar compartment (5-mm thick) with charosphere and soil compartments on both sides. Each charosphere compartment was further divided into five discrete sections (2-mm thick) by PVC sheets with nylon mesh (126 × 158 mm, pore size = 25 μm), which allowed us to separate the biochar/soil zones, but permit the transfer of water-soluble substances and soil microbes across zones. This design enabled soil sampling from six defined zones within the charosphere/soil compartments: 2, 4, 6, 8, 10 and > 10 mm. A small water outlet with nylon mesh for each compartment remained closed at all times, except for periods when leachate was collected prior to destructive soil sampling. This leaching process simulated the lateral diffusion of water and dissolved constituents under field conditions.

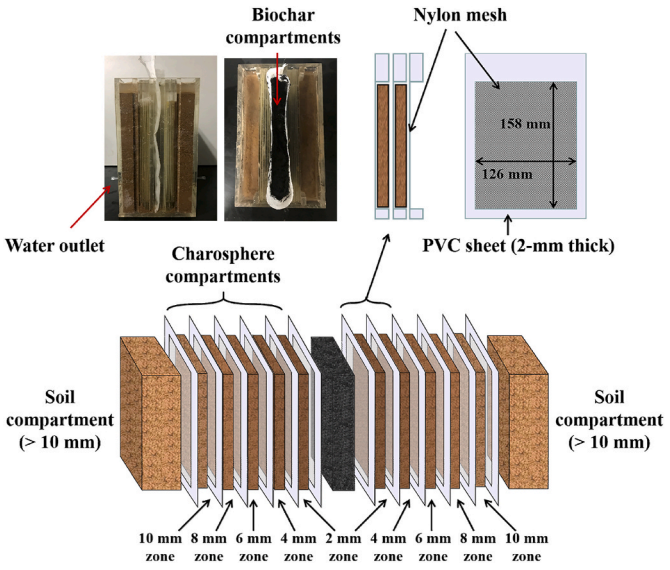

Fig. 1. Schematic of the multi-layer box including 2, 4, 6, 8, 10 mm (2-mm thick) and >10 mm charosphere sub-zones separated by nylon mesh (pore size = 25 μm). Dimension: 150 × 100 × 200 (length × width × height in mm).

Table 1
Selected physicochemical properties of the three biochars used in this study (Means ± S.E., n = 3). Different letters indicate significant differences between treatments ($p < 0.05$).

Biochar type	pH	Dissolved Organic C (g kg^{-1})	Element contents (g kg^{-1})				C/N	C/H	Surface area (m^2 g^{-1})	Pore volume (cm^3 kg^{-1})
			C	H	N	S				
Pristine biochar	8.6 ± 0.0 a	4.9 ± 0.3 a	502 ± 3 a	28 ± 0 ab	31 ± 0 a	2.1 ± 0.0 a	16 ± 0 a	18 ± 0 a	6.8 ± 0.2 c	18 ± 1 b
Acid-modified biochar	7.3 ± 0.1 c	4.4 ± 0.1 a	504 ± 1 a	30 ± 1 a	33 ± 1 a	2.2 ± 0.1 a	15 ± 0 a	17 ± 0 a	7.9 ± 0.3 b	25 ± 2 a
Washed biochar	8.2 ± 0.0 b	0.9 ± 0.0 b	467 ± 2 b	26 ± 1 b	35 ± 2 a	1.2 ± 0.2 a	13 ± 1 b	18 ± 1 a	8.8 ± 0.3 a	21 ± 2 ab

Prior to incubation, 75 mg N kg^{-1} soil of urea (equivalent to 180 kg N ha^{-1}, a common usage rate) was thoroughly mixed with air-dried soil. Each section in the charosphere zone was filled with 60 g of soil and 0.5 kg of soil was added to the soil compartment. The central biochar compartment was filled with 20 g biochar (pristine, acid-modified or washed biochar), or quartz sand as the control, contained in nylon mesh bags (pore size = 25 μm) to prevent the floating/transfer of biochar particles. Deionized water was added to the central compartment of all treatments and maintained at a level 3 cm above the soil surface to retain waterlogged conditions throughout the incubation. Soil was incubated in the dark at 25–28 °C for 7, 14, 28, 49 and 70 days (4 treatments × 3 replicates × 5 sampling times = 60 boxes total). Before soil collection, the water outlets for each soil compartment were opened and 10 mL of leachate was collected. For soil destructive sampling, the six PVC sheets with nylon mesh were extracted from the box together with the soil contained between the two sheets, and soils from each section (2, 4, 6, 8, 10 mm or >10 mm) on both sides of the central biochar compartment were combined as a composite sample for analyses.

2.3. N_2O and CO_2 measurements and chemical analyses

Since we could not collect gas from individual charosphere sections/zones separately during the incubation, the gas emissions were measured immediately after destructive sampling. A 5-g subsample of fresh soil from each of the six zones was transferred to a 30-ml vial and immediately sealed with a rubber septum. The ambient conditions, particularly oxygen level, for these gas measurements unavoidably differed from the *in situ* conditions during incubation. Nevertheless, the measurements provided a potential gas emission metric. Two gas samples (0 and 6 h after sealing) were taken from the vial and injected into 7-mL evacuated serum vials. Concentrations of N_2O and CO_2 were measured using gas chromatography (GC-2010 Plus Shimadzu, Japan). The gas emission rate was calculated as follows:

$$R=(c_6\text{-}c_0) \times V \times M/[24.5 \times T \times m/(1 + w)]$$

where R is the emission rate, c_0 and c_6 are the concentrations of gas at 0 and 6 h, V is the volume of the incubation vial, M is the molecular weight of gas, T is the time interval, m is the mass of fresh soil, and w is the soil moisture content.

Surface area and pore volume of biochar samples were determined by N_2-adsorption/desorption isotherms at 77 K (3 Flex, Micromeritics Instrument, USA). Biochar was degassed for 12 h under vacuum at 200 °C before measurements (Qiu et al., 2017). The pH of soil (1:2.5 w/v) and biochar (1:20 w/v) were measured in deionized water (Yang et al., 2019). The elemental composition of soil and biochars was determined with a CNS analyzer (CNS, 2000; LECO, USA; Yu et al., 2020a). Dissolved organic C (DOC) and N (DON) concentrations were determined in water extracts (soil: 1:5 w/w; biochar: 1:20 w/w; passed through 0.45-μm filters) via a TOC analyzer (Multi N/C 3100 HT1300, Analytik Jena AG, Germany) (Dai et al., 2014). Fresh soil subsamples were used to estimate microbial biomass C by chloroform fumigation-K_2SO_4 extraction (Vance et al., 1987). Briefly, 20 g fresh soil was fumigated in $CHCl_3$ for 24 h and both fumigated and non-fumigated soils were then extracted with 0.5 M K_2SO_4. The organic C in the extracts was determined via a TOC analyzer. The concentrations of NH_4^+-N and NO_3^--N in soil extracts (1 M KCl) and leachates were determined by indophenol blue-ultraviolet colorimetry (Evolution 201, Thermo Scientific, USA) (Yu et al., 2019). Soil urease activity was measured immediately after soil sampling by phenol-sodium hypochlorite colorimetry (Huang, 2012).

2.4. Illumina high-throughput sequencing

Fresh soil (0.5 g) from the 2, 6, 10 and > 10 mm charosphere/soil zones following 7, 28 and 70 days of incubation (4 treatments × 4 zones × 3 replicates × 3 time periods = 144 samples total) was used to extract DNA with a Fast DNA® SPIN Kit for Soil (Qbiogene, USA). DNA was quantified by a Nanodrop® ND-2000 UV–vis spectrophotometer (NanoDrop Technologies, USA). The V4–V5 region of the bacterial 16S rRNA gene was amplified with 515F (5′-GTGCCAGCMGCCGCGGTAA-3′) and 907R (5′-CCGTCAATTCCTTTGAGTTT-3′) primers (Harris et al., 2004). Barcodes (AACGTGAT, GGTGCGAA) were linked with the 5′ end of both primers. Each sample was amplified in a 30-μL system containing 15 μL of Phusion® High-Fidelity PCR Master Mix (New England Biolabs), 3 μL of primers (2 μM), 10 μL sample DNA and 2 μL of ddH_2O. The PCR consisted of 98 °C for 1 min, then 30 cycles at 98 °C for 10 s, 50 °C for 30 s, 72 °C for 30 s, and a final extension at 72 °C for 5 min. Amplified samples were purified and sequencing libraries were generated using the TruSeq DNA PCR-Free Library Preparation Kit (Illumina, USA). The library quality was assessed on a Qubit 2.0 Fluorometer (Thermo Scientific) and Agilent Bioanalyzer 2100 system. Finally, the library was sequenced with a Novaseq 6000 PE250 sequencing platform (Illumina, USA). The amplification, library preparation and high-throughput sequencing processes were completed by Beijing Genomics Institute, China. Sequences were submitted to the Genome Sequence Archive (GSA) database under accession number CRA003521.

Raw data were merged by FLASH (Magoc and Salzberg, 2011). Then, the sequences were quality-filtered (the maximum expected error threshold was 1.0), and chimeras were removed using USEARCH (v 11.0). Operational taxonomic units (OTUs) were defined and clustered using a 97% sequence identity criterion with Uparse (Edgar, 2013). The most frequent sequence for each OTU was picked as the representative sequence. Naive Bayes classifiers (Bokulich et al., 2018) was used to annotate taxonomy for each representative sequence based on SILVA-132 database (v 2020.02) (Caporaso et al., 2010) using QIIME2 platform. All sequencing data were rarefied to a minimum sequencing depth of 27,000 reads.

2.5. Statistical analysis

Permutational multivariate analysis of variance (PERMANOVA) based on Bray-Curtis distance was performed to evaluate the effect of biochar type, incubation time and charosphere zone on bacterial community structure. A Mantel test assessed correlations between soil properties (based on Euclidean distance) and bacterial community composition (based on Bray-Curtis distance). Bray-Curtis similarity coefficients were calculated among samples and visualized using non-metric multidimensional scaling (NMDS). Chao1, Shannon index, PERMANOVA, Mantel test and NMDS were performed using the R package "vegan" (Oksanen et al., 2007). Differential abundance analysis of OTUs was conducted using the R package 'DESeq2' (Differential OTUs between 7 and 70 days, pristine biochar and control, and 2 and 10 mm) (Love et al., 2014) or "edgeR" (differential OTUs among biochars) (Caporaso et al., 2010). *P*-values were adjusted for multiple-testing correction using the Benjamini-Hochberg false discovery rate (FDR) procedure (Benjamini and Hochberg, 1995). The values of adjusted-$p <$ 0.05 were taken as statistically significant.

We used linear discriminant analysis (LDA) with effect size (LEfSe) analysis to determine representative biomarkers (specific abundant taxa) for different groups in various charosphere zones by employing the online tool at http://huttenhower.sph.harvard.edu/galaxy (Segata et al., 2011). The factorial Kruskal-Wallis test assessed differences among treatments using an alpha value of 0.05. The threshold for the logarithmic LDA score for discriminative features was set to 2.0. Statistical differences for N-cycling functional genera were analyzed and plotted with Statistical Analysis of Metagenomic Profiles (STAMP, v 2.1.3) (Parks et al., 2014). Additional plots were created with "ggplot2" in R (v 3.6.2) or OriginPro (v 9.0). One-way analysis of variance (ANOVA) was followed by Turkey's honestly significant difference (HSD) test to assess differences among biochar properties. Two-way

ANOVA (treatments, sampling zones) with Turkey's HSD was performed to test for treatment effects on soil properties. A $p < 0.05$ was considered as statistically significant.

3. Results

3.1. Soil N transformations

Accumulation of NH_4^+ in the 2- and 10-mm zones with pristine biochar was distinctly higher than that with the control and washed biochar until the 28 d of the incubation (Fig. 2A and Table S1). Meanwhile, NH_4^+ concentration in the control progressively increased until reaching a plateau at 49 d. Differences in NH_4^+ with respect to distance from the biochar source were recorded before 28 d for all three biochar types. The NH_4^+ concentrations were 1.3-, 2.9- and 1.8-fold higher in the 2-mm versus 10-mm zone at 7 d in the pristine, acid-modified and washed biochar treatments ($p < 0.05$), respectively, whereas it did not differ among sampling zones in the control. The highest concentration of NO_3^--N (30 mg kg^{-1}) was found in the control, which decreased gradually with increasing incubation time (Fig. 2B). Contrary to NH_4^+, NO_3^- concentrations were 3.3- and 1.7-fold higher in 10-mm zone than 2-mm zone of the acid-modified biochar and washed biochar treatments at 7 d ($p < 0.05$, Table S1). Soil with pristine biochar contained lower NO_3^- concentrations (<5 mg kg^{-1}) than other treatments. Concentrations of NH_4^+ and NO_3^- in leachates of pristine biochar were consistently lower among all the treatments, except NH_4^+ at 14 d (Fig. S1). The peak NO_3^--N concentration was 45 mg L^{-1} in leachates from the control at 28 d, followed by 39, 33 and 9 mg L^{-1} with washed, acid-modified and pristine biochar, whereas NH_4^+ concentration was lower in the control than in the acid-modified and washed biochar treatments all the time.

Emissions of N_2O generally decreased over time (Fig. 2C). No emissions were recorded after 28 d for the three biochar treatments, whereas N_2O emission persisted until 49 d in the control. The pristine biochar significantly decreased N_2O emission at 7 and 14 d compared to the control, acid-modified and washed biochars.

There was a substantial increase of urease activities in the 2-mm zone with pristine biochar compared to those in the control, acid-modified and washed biochars ($p < 0.05$, Fig. 2D, Table S1). Urease activities with pristine biochar were 4.2- and 2.9-fold higher in the 2-mm versus 10-mm zone at 7 and 14 d, respectively. Peak urease activities reached 38 mmol N kg^{-1} d^{-1} in the 2-mm zone at 7 d.

3.2. Alteration of soil bacterial community

The α-diversity significantly increased over time for all biochar treatments, as well as the control (Fig. 3A and S4). At 7 d, Chao1 and Shannon indices in the 6, 10 and > 10 mm zones showed no statistical difference across biochar treatments, whereas α-diversity in the 2-mm zone was highest with the washed biochar, followed by the acid-modified biochar, control and pristine biochar. At 70 d, Shannon indices decreased with increasing distance from the acid-modified and washed biochar sources, but no difference was found for pristine biochar.

PERMANOVA examined variations in the bacterial community with respect to biochar type, incubation time and charosphere zone, both individually and in combination (Table S2). Incubation time explained the largest portion of the variation (39.7%, $p < 0.001$), followed by the distance from the biochar source (14.1%, $p < 0.001$) and biochar type (12.1%, $p < 0.001$). Furthermore, a Mantel test revealed that edaphic parameters significantly affected bacterial community structure, including pH ($p < 0.01$), DOC ($p < 0.01$), DON ($p < 0.01$), NH_4^+ ($p < 0.01$), NO_3^- ($p < 0.01$) and N_2O emission ($p < 0.05$) (Table 2). NMDS ordination showed a clear separation of the bacterial communities between 7 and 70 d across the first principal coordinate (Fig. 3B). Biochar type and sampling zone also contributed to the variation, especially at 7 d. The variation in the distance effect weakened over time with pristine biochar distinctly separated from the other biochar treatments.

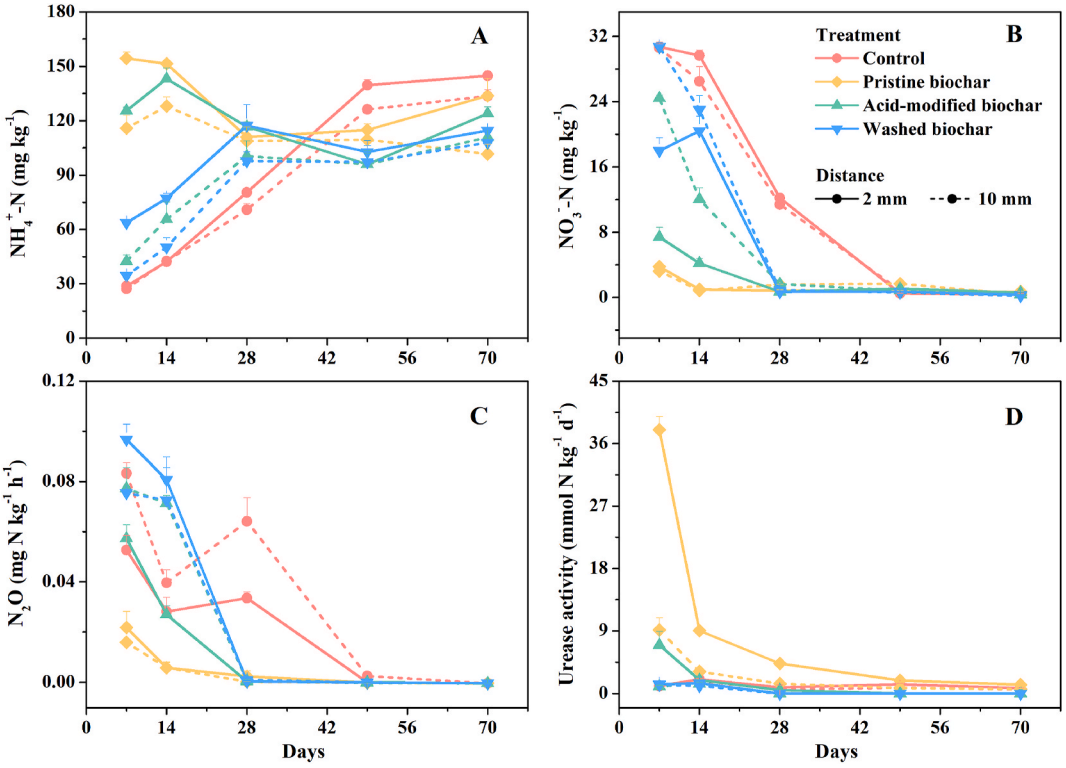

Fig. 2. Concentrations of NH_4^+-N (A) and NO_3^--N (B), N_2O emissions (C) and urease activities (D) in the 2- and 10-mm charosphere zones during 70 d of incubation. Error bars indicate the standard error of three replicates.

Table 2
Mantel correlations between bacterial diversity and soil chemical properties.

Soil properties	R	*p*-value[a]
pH	0.366	<0.001
Dissolved organic C	0.242	<0.001
Dissolved organic N	0.320	<0.001
NH_4^+	0.289	<0.001
NO_3^-	0.168	<0.001
Microbial biomass C	0.0149	0.286
N_2O emission	0.093	0.016
Urease activity	−0.041	0.827

[a] *p*-value was derived from 9999 permutations.

3.3. Specific bacterial taxa modulated by biochar

Compared to the bacterial community composition at 7 d, relative abundances of 1482 OTUs ($p < 0.05$) increased whereas 560 OTUs ($p < 0.05$) declined at 70 d for all treatments and distances (Fig. 4A). The number of enriched OTUs was highest in pristine biochar (265), followed by washed biochar (80) and acid-modified biochar (18) (Fig. 4C). Furthermore, 554 OTUs ($p < 0.05$) were enriched and 552 OTUs ($p < 0.05$) depleted in the pristine biochar treatment relative to the control (Fig. 4B). Differential abundance analysis identified OTUs affected by distance from the biochar source (Fig. 5A). Compared to the 10-mm zone, pristine biochar significantly increased the abundance of 236 OTUs in the 2-mm zone at 70 d, especially those from the phyla Proteobacteria, Firmicutes and Actinobacteria, whereas 118 depleted OTUs were mainly identified as Firmicutes.

LEfSe analysis determined the effect of distance from the biochar source on specific bacterial taxa from the phylum to genus level. A total of 88, 16, 6 and 27 clades were enriched in the 2, 6, 10 and > 10 mm zones, respectively (Fig. 5B). At the class level, significant increases were found for the abundances of Melainabacteria, AD3 and Negativicutes in the 2-mm zone, Cyanobacteria in the 6-mm zone, Coriobacteriia in the 10-mm zone, and Ignavibacteria and Latescibacteria in the >10-mm zone.

3.4. N-cycling functional bacteria in response to biochar

Statistical analysis of metagenomic profiles (STAMP) investigated how specific N-cycling functional genera responded to biochar (Fig. 6). The pristine biochar increased the abundance of *Massilia* ($p < 0.001$), *Anaeromyxobacter* ($p < 0.05$), *Cupriavidus* ($p < 0.01$), *Achromobacter* ($p < 0.05$) and *Janthinobacterium* ($p < 0.01$) by 16.0%, 8.8%, 1.6%, 0.8% and 0.03%, respectively, based on all sampling zones and times. Furthermore, the abundances of genera *Rhodopseudomonas, Rhodanobacter*, *Hydrogenispora* and *Nitrospira* ($p < 0.001$) decreased by 5.2%, 4.4%, 3.8% and 0.1%, respectively (Fig. 6A, Table S3). Compared to the 10-mm zone, *Rhodopseudomonas* was overrepresented in the 2-mm zone of all three biochar types (Fig. 6, Table S4). Both acid-modified and washed biochars increased the abundances of *Sphingomonas*, *Craurococcus*, *Rhizobium*, *Paracoccus* and *Ensifer*, whereas pristine biochar increased the abundances of *Bacillus*, *Methylocystis*, *Methylophilus, Roseomonas* and *MND1*. In contrast, *Massilia* and *Janthinobacterium* were overrepresented in the 10-mm versus 2-mm zone of the pristine biochar treatment.

4. Discussion

4.1. "Unbalanced competition" induced soil bacterial community differentiation in the charosphere

Soil bacterial composition was significantly affected by incubation

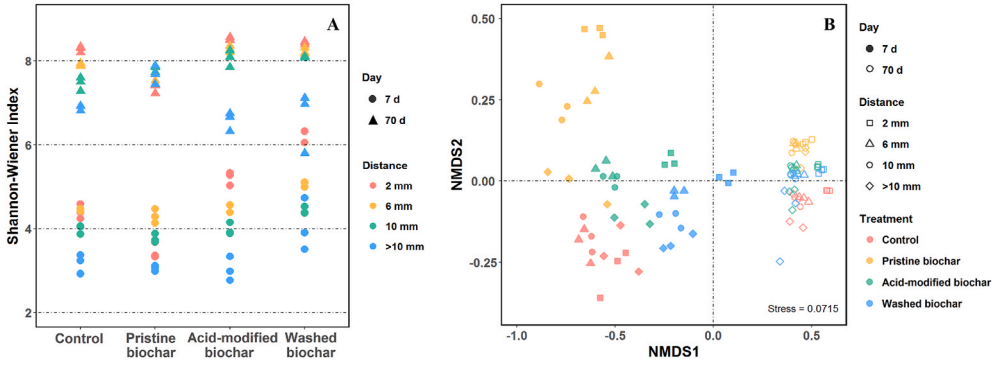

Fig. 3. Bacterial α-diversity as revealed by Shannon-Wiener index (A) and non-metric multidimensional scaling ordination plot (NMDS) based on Bray-Curtis matrix of the soil bacterial community composition (B) in various charosphere zones of the control, pristine biochar, acid-modified biochar and washed biochar treatments after 7 and 70 d of incubation.

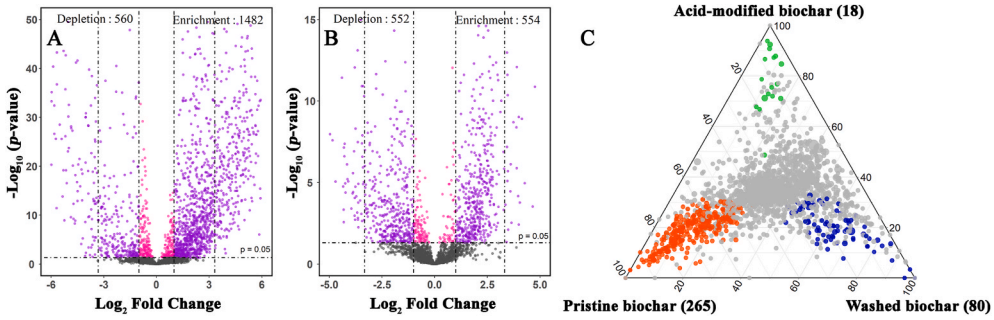

Fig. 4. Volcano plots showing the fold change (x-axis) in differential OTUs, as well as the statistical significance of that change (y-axis). (A) Differential OTUs at 70 d versus 7 d for all treatments and charosphere zones. (B) Differential OTUs with pristine biochar versus control for all sampling times and charosphere zones. Each point represents an individual OTU that increased/decreased more than (purple) or less than (pink) 2-fold. (C) OTU enrichment in pristine biochar (orange), acid-modified biochar (green) and washed biochar (blue) at 70 d. Ternary plot shows the percent of each OTU's occurrence. The values in brackets are the number of significant OTUs in each treatment. (For interpretation of the references to color in this figure legend, the reader is referred to the Web version of this article.)

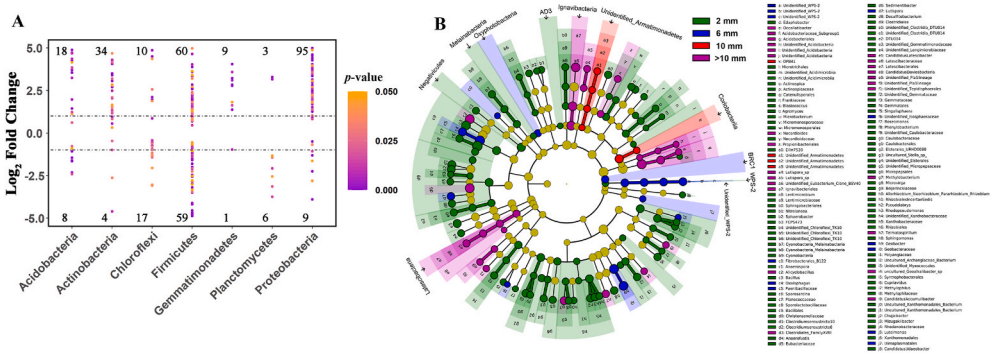

Fig. 5. (A) Enrichment and depletion of bacterial OTUs in the 2-mm versus 10-mm zone with pristine biochar at 70 d from differential abundance analysis. Each point represents a single OTU. Dash lines represent a 2-fold increase/decrease. The numbers represent the number of differential OTUs. (B) Cladogram of linear discriminant analysis with effect size showing discriminative taxa among different charosphere zones with pristine biochar at 70 d. The corresponding node in the taxonomic cladogram is color-coded according to the highest-ranked group for that taxon. The yellow nodes refer the species with no significant difference between charosphere zones. The six rings of the cladogram represent the domain (innermost), phylum, class, order, family and genus. (For interpretation of the references to color in this figure legend, the reader is referred to the Web version of this article.)

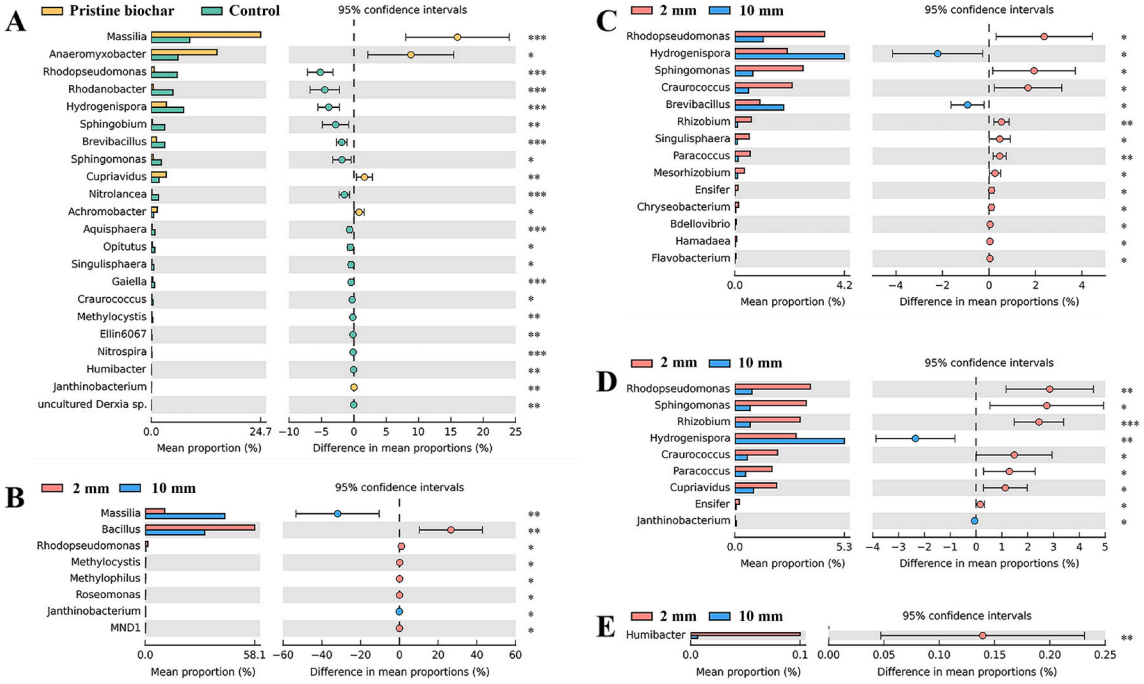

Fig. 6. Variation analysis of bacterial community with pristine biochar versus the control at the genus level with all sampling times and charosphere zones (A). Variation analysis of bacterial community in the 2-mm versus 10-mm zone at the genus level with pristine biochar (B), acid-modified biochar (C), washed biochars (D) and the control (E). *, ** and *** represent significance at $p < 0.05$, $p < 0.01$ and $p < 0.001$, respectively. The *p*-values were adjusted using the Benjamini-Hochberg false discovery rate (FDR) procedure.

time, distance from the biochar source and biochar type (Table S2). Notably, the pristine biochar did not increase the Chao1 and Shannon index compared to the control irrespective of its higher pH and DOC concentration (Figs. S2–3), contrary to several previous studies (Xu et al., 2014; Sheng and Zhu, 2018; Thi et al., 2018), which demonstrates that pristine biochar did not increase the richness and the evenness of the community compared to control. This unexpected result might be attributed to "unbalanced competition", a phenomenon in which the growth of particularly responsive bacterial taxa was promoted by the application of biochar that in turn led to the suppression of other species (Dai et al., 2018a). A selective influence of pristine biochar on bacterial composition is further supported by the differential analysis of OTUs (Fig. 4B). The number of enriched OTUs (554) in the pristine biochar treatment relative to the control was similar to that of depleted OTUs (552). Correspondingly, the bacterial community structure in the pristine biochar treatment showed a clear distinction from the control, acid-modified and washed biochar treatments (Fig. 3B). This demonstrates the selective effect of pristine biochar as a key factor leading to specialization within the bacterial community structure (Wang et al., 2019). This is consistent with Zhang et al. (2021) findings that soil-pyrogenic organic matter heterogeneity was a strong selection factor for microbial assembly. In contrast, the acid-modified and washed biochar treatments significantly increased the Chao1 and Shannon index, suggesting that biochar neutralization or removal of toxic dissolved compounds alleviated the suppression of bacterial species caused by the pristine biochar. For example, toxicity mitigation might result from leaching of furans, polycyclic aromatic hydrocarbons and dioxins that are often presented on biochar (Intani et al., 2019). All this evidence demonstrates that pristine biochar increased the blooming taxa while suppressing others.

In terms of distance from the biochar source, pristine biochar did not result in significant differences in α-diversity among the sampling zones.

This might result from the higher alkalinity and DOC concentrations in the pristine biochar than acid-modified and washed biochar treatments (Table 1). The pH and DOC concentrations were higher in the near-charosphere than outer-charosphere zones of acid-modified and washed biochars at 70 d, whereas there was no significant difference between the sampling zones with pristine biochar (Figs. S2–3). Labile nutrients and DOC diffused rapidly across all sampling zones of the pristine biochar treatment leading to a relatively homogenous environment (pH and C source) for bacteria compared to the acid-modified and washed biochar treatments. In contrast to α-diversity, the responsive bacterial species were more abundant in the 2-mm zone compared to the other sampling zones (Fig. 5), indicating that pristine biochar altered the bacterial composition more strongly in the 2-mm zone, but did not affect the overall species diversity, which also supports the "unbalanced competition" concept.

At 70 d, phylum Proteobacteria typically had a higher abundance in the 2- versus 10-mm zone in the pristine biochar treatment even though the α-diversity did not show much difference (Fig. 5A). The differences between enriched and depleted OTUs from other phyla were less than Proteobacteria. Dai et al. (2016) reported that pyrogenic organic matter contributed a large amount of easily-mineralizable C, leading to an enrichment of Proteobacteria that are highly responsive to nutrient inputs and consume more labile forms of C (Fierer et al., 2007; Yu et al., 2020b). Meanwhile, rapid urea hydrolysis with pristine biochar addition provided a large amount of NH_4^+ at the beginning of the incubation due to more favorable pH conditions for urease activity (Fisher et al., 2017). This is supported by the lower urease activities in the acid-modified and washed biochars versus pristine biochar treatment (Fig. 2) owing to the lower pH in the acid-modified and washed biochar treatments (Fig. S2). Higher NH_4^+ concentration was one reason for the increased abundance of Proteobacteria. The alleviation of N limitation allowed the N-cycling functional species to effectively outcompete the others (Li et al., 2016). Several species of Proteobacteria are involved in N-cycling processes, which displayed increased abundance in the 2-mm zone of the pristine biochar treatment, further altering soil bacterial functions (Spain et al., 2009).

4.2. Spatial variation in distribution of N-cycling functional across the charosphere

The abundances of species responsible for N-cycling, mostly from the Proteobacteria, were higher in the 2-mm versus 10-mm zone (Fig. 6 and Table S4). Proteobacteria were highly responsive to N concentrations and comprised the most dominant groups functioning in nitrification, denitrification and N_2-fixation (Guo et al., 2020; Solanki et al., 2020). Dai et al. (2018b) reported that increased supply of organic C and nutrients was more important in determining the abundance and composition of Proteobacteria than soil pH. Although pristine biochar decreased some of the species involved in N-cycling compared to the control (Fig. 6A), many specific genera were enriched in the 2-mm zone relative to the 10-mm zone of the pristine biochar treatment (Fig. 6B–D). Thus, the spatial variation in distribution of N-cycling functional species altered N-cycling processes with distance across the charosphere.

MND1, belonging to the family *Nitrosomonadaceae*, was enriched in the 2-mm zone and represents taxonomic units comprising ammonia-oxidizing bacteria (Kong et al., 2016). The abundance of genera *Nitrospira* and *Nitrolancea*, responsible for NO_2^- oxidization (Spieck et al., 2020) decreased in the pristine biochar treatment, but did not show any differences between the 2- and 10-mm zones. Moreover, the full nitrification process ($NH_4^+ \rightarrow NO_2^- \rightarrow NO_3^-$) can be completed by some species of *Nitrospira*, making the *Nitrospira* genus a key component of the N-cycling bacterial community (van Kessel et al., 2015; Zhang et al., 2017). Han et al. (2017) also reported that biochar decreased the abundance of the *Nitrospira* genus in continuously cropped soils. The lower abundances of genera *Nitrospira* and *Nitrolancea* implied that pristine biochar decreased the nitrification potential. In addition, the higher urease activities and NH_4^+ concentration combined with the lower NO_3^- concentration in the pristine biochar treatment indicated that pristine biochar decreased the oxidization of NH_4^+ to NO_3^- (Fig. 2).

Correspondingly, denitrification potential was reduced due to the lower concentration of NO_3^- in the pristine biochar treatment (Fig. 2B). Some genera for denitrification, such as *Methylocystis* (Dam et al., 2013) and *Paracoccus* (Virdis et al., 2011), had lower abundances in the 10-mm zone. The *nosZ* gene for N_2O reduction to N_2 has been detected in genera *Anaeromyxobacter* and *Rhodopseudomonas* (Orellana et al., 2014). Notably, we found that pristine biochar increased the abundance of *Anaeromyxobacter*, but decreased that of *Rhodopseudomonas*, whereas *Rhodopseudomonas* was over-represented in the 2-mm versus 10-mm zone of all three biochar types. Even though biochar selectively decreased some N-cycling functional taxa, it still provided a suitable habitat in the near-charosphere zone regardless of whether dissolved constituents were removed. We posit that biochar was responsible for the distinct distribution of species involved in N cycle, but this study could not determine the dominant factor driving the alteration.

Some species of genera *Bacillus* (Yousuf et al., 2017), *Cupriavidus* (Liu et al., 2012), *Rhizobium* (Masson-Boivin et al., 2009), *Mesorhizobium* (Gerding et al., 2012) and *Ensifer* (Ardley, 2017) are involved in N_2-fixation. However, most of these genera, except *Bacillus*, are symbiotic N_2-fixing species. Since N_2-fixation was observed to be inhibited by high NH_4^+ concentrations and the NH_4^+ concentrations were positively correlated with urease activities (Fig. S5, $R^2 = 0.87$, $p < 0.0001$), the accumulation of NH_4^+ in the 2-mm zone of pristine biochar treatments is attributed to the high urease activity. The enrichment of *Massilia* with pristine biochar may be related to its high proliferation rates when sufficient C is available as an energy source (Li et al., 2014). The genus *Massilia* has the ability to produce urease and reduce nitrate (Zhang et al., 2006; Zu et al., 2008), consistent with the increased urease activities in the pristine biochar treatments (Fig. 2D). However, *Massilia* abundance was much lower in the 2- versus 10-mm zone of the pristine biochar treatment, indicating a potential tolerance limit of *Massilia* to biochar-induced changes.

Previous studies largely neglected the spatial variability of soil microorganisms across soil-biochar gradients. Our study rigorously elucidated a distance-decay relationship of biochar-induced microbial responses across the charosphere under waterlogged conditions. Therefore, the N-cycling processes differed along the charosphere gradient. We demonstrated that biochar did not promote soil bacterial diversity (as revealed by the Chao1 and Shannon index), but did alter community composition, which was attributed to "unbalanced competition" between biochar-promoted and biochar-suppressed taxa. The Proteobacteria were enriched in the charosphere; it was highly responsive to N supply and comprised the most dominant species functioning in N-cycling processes. Although biochar decreased some specific genera related to N-cycling, some species responsible for N_2 fixation, ammonia oxidization and denitrification were still enriched in the near-charosphere zone compared to the outer-charosphere. Hence, the spatial distribution of some specific species had altered functional traits with distance across the charosphere. This study elucidates the spatial relationship between N distribution and bacterial functions within the charosphere under waterlogged conditions. It improves our understanding of how biochar regulates soil N-cycling. Future work should be devoted to examining the spatial heterogeneity of biochar effects on agricultural N management, especially for mitigating N losses from NO_3^- leaching and denitrification.

Declaration of competing interest

The authors declare that they have no known competing financial interests or personal relationships that could have appeared to influence the work reported in this paper.

Acknowledgements

We thank Yuanhao Wang for his valuable contribution to this research. This work was supported by the National Natural Science Foundation of China (41721001, 41520104001), 111 Project (B17039), and Fundamental Research Funds for Central Universities in China.

Appendix A. Supplementary data

Supplementary data to this article can be found online at https://doi.org/10.1016/j.soilbio.2021.108420.

References

Ardley, J., 2017. Legumes of the Thar Desert and their nitrogen fixing *Ensifer* symbionts. Plant and Soil 410, 517–520.

Benjamini, Y., Hochberg, Y., 1995. Controlling the false discovery rate - a practical and powerful approach to multiple testing. Journal of the Royal Statistical Society: Series B 57, 289–300.

Bokulich, N.A., Kaehler, B.D., Rideout, J.R., Dillon, M., Bolyen, E., Knight, R., Huttley, G. A., Caporaso, J.G., 2018. Optimizing taxonomic classification of marker-gene amplicon sequences with QIIME 2's q2-feature-classifier plugin. Microbiome 6, 90.

Caporaso, J.G., Kuczynski, J., Stombaugh, J., Bittinger, K., Bushman, F.D., Costello, E.K., Fierer, N., Pena, A.G., Goodrich, J.K., Gordon, J.I., Huttley, G.A., Kelley, S.T., Knights, D., Koenig, J.E., Ley, R.E., Lozupone, C.A., McDonald, D., Muegge, B.D., Pirrung, M., Reeder, J., Sevinsky, J.R., Tumbaugh, P.J., Walters, W.A., Widmann, J., Yatsunenko, T., Zaneveld, J., Knight, R., 2010. QIIME allows analysis of high-throughput community sequencing data. Nature Methods 7, 335–336.

Dai, Z., Enders, A., Rodrigues, J.L.M., Hanley, K.L., Brookes, P.C., Xu, J., Lehmann, J., 2018a. Soil fungal taxonomic and functional community composition as affected by biochar properties. Soil Biology and Biochemistry 126, 159–167.

Dai, Z., Hu, J., Xu, X., Zhang, L., Brookes, P.C., He, Y., Xu, J., 2016. Sensitive responders among bacterial and fungal microbiome to pyrogenic organic matter (biochar) addition differed greatly between rhizosphere and bulk soils. Scientific Reports 6, 36101.

Dai, Z., Su, W., Chen, H., Barberán, A., Zhao, H., Yu, M., Yu, L., Brookes, P.C., Schadt, C. W., Chang, S.X., Xu, J., 2018b. Long-term nitrogen fertilization decreases bacterial diversity and favors the growth of Actinobacteria and Proteobacteria in agro-ecosystems across the globe. Global Change Biology 24, 3452–3461.

Dai, Z., Wang, Y., Muhammad, N., Yu, X., Xiao, K., Meng, J., Liu, X., Xu, J., Brookes, P.C., 2014. The effects and mechanisms of soil acidity changes, following incorporation of biochars in three soils differing in initial pH. Soil Science Society of America Journal 78, 1606–1614.

Dai, Z., Xiong, X., Zhu, H., Xu, H., Leng, P., Li, J., Tang, C., Xu, J., 2021. Association of biochar properties with changes in soil bacterial, fungal and fauna communities and nutrient cycling processes. Biochar 3, 239–254.

Dam, B., Dam, S., Blom, J., Liesack, W., 2013. Genome analysis coupled with physiological studies reveals a diverse nitrogen metabolism in *Methylocystis* sp. strain SC2. PloS One 8, e74767.

Edgar, R.C., 2013. UPARSE: highly accurate OTU sequences from microbial amplicon reads. Nature Methods 10, 996–998.

Fisher, K.A., Yarwood, S.A., James, B.R., 2017. Soil urease activity and bacterial *ureC* gene copy numbers: effect of pH. Geoderma 285, 1–8.

Fierer, N., Bradford, M.A., Jackson, R.B., 2007. Toward an ecological classification of soil bacteria. Ecology 88, 1354–1364.

Gerding, M., O'Hara, G.W., Braeu, L., Nandasena, K., Howieson, J.G., 2012. Diverse *Mesorhizobium* spp. with unique *nodA* nodulating the South African legume species of the genus *Lessertia*. Plant and Soil 358, 385–401.

Gosz, J.R., 1993. Ecotone hierarchies. Ecological Applications 3, 369–376.

Gul, S., Whalen, J.K., 2016. Biochemical cycling of nitrogen and phosphorus in biochar-amended soils. Soil Biology and Biochemistry 103, 1–15.

Guo, H., Gu, J., Wang, X., Nasir, M., Yu, J., Lei, L., Wang, J., Zhao, W., Dai, X., 2020. Beneficial effects of bacterial agent/bentonite on nitrogen transformation and microbial community dynamics during aerobic composting of pig manure. Bioresource Technology 298, 122384.

Han, G., Lan, J., Chen, Q., Yu, C., Bie, S., 2017. Response of soil microbial community to application of biochar in cotton soils with different continuous cropping years. Scientific Reports 7, 1–11.

Harris, J.K., Kelley, S.T., Pace, N.R., 2004. New perspective on uncultured bacterial phylogenetic division OP11. Applied and Environmental Microbiology 70, 845–849.

Huang, J., 2012. The Effect of Biochar Application on Soil Microbial Biomass and Soil Enzymes. Chinese Academy of Agricultural Science, Beijing.

Intani, K., Latif, S., Islam, M.S., Mueller, J., 2019. Phytotoxicity of corncob biochar before and after heat treatment and washing. Sustainability 11, 30.

Karppinen, E.M., Mamet, S.D., Stewart, K.J., Siciliano, S.D., 2019. The charosphere promotes mineralization of ^{13}C-phenanthrene by psychrotrophic microorganisms in Greenland soils. Journal of Environmental Quality 48, 559–567.

Kolasa, J., Zalewski, M., 1995. Notes on ecotone attributes and functions. Hydrobiologia 303, 1–7.

Kong, Q., Wang, Z., Niu, P., Miao, M., 2016. Greenhouse gas emission and microbial community dynamics during simultaneous nitrification and denitrification process. Bioresource Technology 210, 94–100.

Lam, S.K., Suter, H., Mosier, A.R., Chen, D., 2017. Using nitrification inhibitors to mitigate agricultural N_2O emission: a double-edged sword? Global Change Biology 23, 485–489.

Lehmann, J., Joseph, S., 2015. Biochar for Environmental Management: Science, Technology and Implementation. Routledge.

Li, H., Xu, Z., Yang, S., Li, X., Top, E.M., Wang, R., Zhang, Y., Cai, J., Yao, F., Han, X., Jiang, Y., 2016. Responses of soil bacterial communities to nitrogen deposition and precipitation increment are closely linked with aboveground community variation. Microbial Ecology 71, 974–989.

Li, X., Rui, J., Mao, Y., Yannarell, A., Mackie, R., 2014. Dynamics of the bacterial community structure in the rhizosphere of a maize cultivar. Soil Biology and Biochemistry 68, 392–401.

Liu, Q., Zhang, Y., Liu, B., Amonette, J.E., Lin, Z., Liu, G., Ambus, P., Xie, Z., 2018. How does biochar influence soil N cycle? A meta-analysis. Plant and Soil 426, 211–225.

Liu, X., Wei, S., Wang, F., James, E.K., Guo, X., Zagar, C., Xia, L.G., Dong, X., Wang, Y.P., 2012. *Burkholderia* and *Cupriavidus* spp. are the preferred symbionts of *mimosa* spp. in southern China. FEMS Microbiology Ecology 80, 417–426.

Love, M.I., Huber, W., Anders, S., 2014. Moderated estimation of fold change and dispersion for RNA-seq data with DESeq2. Genome Biology 15, 550.

Luo, Y., Durenkamp, M., De Nobili, M., Lin, Q., Devonshire, B.J., Brookes, P.C., 2013. Microbial biomass growth, following incorporation of biochars produced at 350°C or 700°C, in a silty-clay loam soil of high and low pH. Soil Biology and Biochemistry 57, 513–523.

Ma, B., Stirling, E., Liu, Y., Zhao, K., Zhou, J., Singh, B.K., Tang, C., Dahlgren, R.A., Xu, J., 2021. Soil biogeochemical cycle couplings inferred from a function-taxon network. Research 2021, 7102769.

Magoc, T., Salzberg, S.L., 2011. FLASH: Fast length adjustment of short reads to improve genome assemblies. Bioinformatics 27, 2957–2963.

Masson-Boivin, C., Giraud, E., Perret, X., Batut, J., 2009. Establishing nitrogen-fixing symbiosis with legumes: how many rhizobium recipes? Trends in Microbiology 17, 458–466.

Molina-Herrera, S., Haas, E., Klatt, S., Kraus, D., Augustin, J., Magliulo, V., Tallec, T., Ceschia, E., Ammann, C., Loubet, B., Skiba, U., Jones, S., Bruemmer, C., Butterbach-Bahl, K., Kiese, R., 2016. A modeling study on mitigation of N_2O emissions and NO_3 leaching at different agricultural sites across Europe using LandscapeDNDC. Science of the Total Environment 553, 128–140.

Oksanen, J., Kindt, R., Legendre, P., O'Hara, B., Stevens, M.H.H., Oksanen, M.J., Suggests, M., 2007. The vegan package. Community Ecology Package 10, 719.

Orellana, L.H., Rodriguez-R, L.M., Higgins, S., Chee-Sanford, J.C., Sanford, R.A., Ritalahti, K.M., Loeffler, F.E., Konstantinidis, K.T., 2014. Detecting nitrous oxide reductase (*nosZ*) genes in soil metagenomes: method development and implications for the nitrogen cycle. mBio 5 e01193-14.

Parks, D.H., Tyson, G.W., Hugenholtz, P., Beiko, R.G., 2014. STAMP: statistical analysis of taxonomic and functional profiles. Bioinformatics 30, 3123–3124.

Pei, J., Zhuang, S., Cui, J., Li, J., Li, B., Wu, J., Fang, C., 2017. Biochar decreased the temperature sensitivity of soil carbon decomposition in a paddy field. Agriculture, Ecosystems & Environment 249, 156–164.

Peterson, C.A., Brown, R.C., 2020. Oxidation kinetics of biochar from woody and herbaceous biomass. Chemical Engineering Journal 401, 126043.

Pingree, M.R.A., DeLuca, T.H., 2017. Function of wildfire-deposited pyrogenic carbon in terrestrial ecosystems. Frontiers in Environmental Science 5, 53.

Pokharel, P., Ma, Z., Chang, S.X., 2020. Biochar increases soil microbial biomass with changes in extra- and intracellular enzyme activities: a global meta-analysis. Biochar 2, 65–79.

Qiu, C., He, Y., Brookes, P., Xu, J., 2017. The systematic characterization of nanoscale bamboo charcoal and its sorption on phenanthrene: a comparison with microscale. Science of the Total Environment 578, 399–407.

Quilliam, R.S., Glanville, H.C., Wade, S.C., Jones, D.L., 2013. Life in the 'charosphere' - does biochar in agricultural soil provide a significant habitat for microorganisms? Soil Biology and Biochemistry 65, 287–293.

Segata, N., Izard, J., Waldron, L., Gevers, D., Miropolsky, L., Garrett, W.S., Huttenhower, C., 2011. Metagenomic biomarker discovery and explanation. Genome Biology 12, 1–28.

Sheng, Y., Zhu, L., 2018. Biochar alters microbial community and carbon sequestration potential across different soil pH. Science of the Total Environment 622, 1391–1399.

Solanki, M.K., Wang, Z., Wang, F., Li, C., Gupta, C.L., Singh, R.K., Malviya, M.K., Singh, P., Yang, L., Li, Y., 2020. Assessment of diazotrophic *Proteobacteria* in sugarcane rhizosphere when intercropped with legumes (peanut and soybean) in the field. Frontiers in Microbiology 11, 1814.

Spain, A.M., Krumholz, L.R., Elshahed, M.S., 2009. Abundance, composition, diversity and novelty of soil *Proteobacteria*. The ISME Journal 3, 992–1000.

Spieck, E., Sass, K., Keuter, S., Hirschmann, S., Spohn, M., Indenbirken, D., Kop, L.F.M., Luecker, S., Giaveno, A., 2020. Defining culture conditions for the hidden nitrite-oxidizing bacterium *Nitrolancea*. Frontiers in Microbiology 11, 1522.

Thi, T.N.N., Wallace, H.M., Xu, C., Zwieten, L.V., Weng, Z.H., Xu, Z., Che, R., Tahmasbian, I., Hu, H., Bai, S.H., 2018. The effects of short term, long term and reapplication of biochar on soil bacteria. Science of the Total Environment 636, 142–151.

van Kessel, M.A.H.J., Speth, D.R., Albertsen, M., Nielsen, P.H., Op Den Camp, H.J.M., Kartal, B., Jetten, M.S.M., Lucker, S., 2015. Complete nitrification by a single microorganism. Nature 528, 555.

Vance, E.D., Brookes, P.C., Jenkinson, D.S., 1987. An extraction method for measuring soil microbial biomass C. Soil Biology and Biochemistry 19, 703–707.

Virdis, B., Read, S.T., Rabaey, K., Rozendal, R.A., Yuan, Z., Keller, J., 2011. Biofilm stratification during simultaneous nitrification and denitrification (SND) at a biocathode. Bioresource Technology 102, 334–341.

Wang, R., Wei, S., Jia, P., Liu, T., Hou, D., Xie, R., Lin, Z., Ge, J., Qiao, Y., Chang, X., Lu, L., Tian, S., 2019. Biochar significantly alters rhizobacterial communities and reduces Cd concentration in rice grains grown on Cd-contaminated soils. Science of the Total Environment 676, 627–638.

Xu, H., Wang, X., Li, H., Yao, H., Su, J., Zhu, Y., 2014. Biochar impacts soil microbial community composition and nitrogen cycling in an acidic soil planted with rape. Environmental Science and Technology 48, 9391–9399.

Yang, X., Tsibart, A., Nam, H., Hur, J., El-Naggar, A., Tack, F.M.G., Wang, C., Lee, Y.H., Tsang, D.C.W., Ok, Y.S., 2019. Effect of gasification biochar application on soil quality: trace metal behavior, microbial community, and soil dissolved organic matter. Journal of Hazardous Materials 365, 684–694.

Yousuf, J., Thajudeen, J., Rahiman, M., Krishnankutty, S., Alikunj, A.P., Abdulla, M.H.A., 2017. Nitrogen fixing potential of various heterotrophic *Bacillus* strains from a tropical estuary and adjacent coastal regions. Journal of Basic Microbiology 57, 922–932.

Yu, L., Homyak, P.M., Kang, X., Brookes, P.C., Ye, Y., Lin, Y., Muhammad, A., Xu, J., 2020a. Changes in abundance and composition of nitrifying communities in barley (*Hordeum vulgare* L.) Rhizosphere and bulk soils over the growth period following combined biochar and urea amendment. Biology and Fertility of Soils 56, 169–183.

Yu, M., Meng, J., Yu, L., Su, W., Afzal, M., Li, Y., Brookes, P.C., Redmile-Gordon, M., Luo, Y., Xu, J., 2019. Changes in nitrogen related functional genes along soil pH, C and nutrient gradients in the charosphere. Science of the Total Environment 650, 626–632.

Yu, M., Su, W.Q., Parikh, S.J., Li, Y., Tang, C., Xu, J., 2021. Intact and washed biochar caused different patterns of nitrogen transformation and distribution in a flooded paddy soil. Journal of Cleaner Production 293, 126259.

Yu, Z., Ling, L., Singh, B.P., Luo, Y., Xu, J., 2020b. Gain in carbon: deciphering the abiotic and biotic mechanisms of biochar-induced negative priming effects in contrasting soils. Science of the Total Environment 746, 141057.

Yue, H., Zhang, Y., He, Y., Wei, G., Shu, D., 2019. Keystone taxa regulate microbial assemblage patterns and functional traits of different microbial aggregates in simultaneous anammox and denitrification (SAD) systems. Bioresource Technology 290, 121778.

Zhang, K., Chen, L., Li, Y., Brookes, P.C., Xu, J., Luo, Y., 2017. The effects of combinations of biochar, lime, and organic fertilizer on nitrification and nitrifiers. Biology and Fertility of Soils 53, 77–87.

Zhang, L., Jing, Y., Xiang, Y., Zhang, R., Lu, H., 2018. Responses of soil microbial community structure changes and activities to biochar addition: a meta-analysis. Science of the Total Environment 643, 926–935.

Zhang, L., Ma, B., Tang, C., Yu, H., Lv, X., Rodrigues, J.L.M., Dahlgren, R.A., Xu, J., 2021. Habitat heterogeneity induced by pyrogenic organic matter in wildfire-perturbed soils mediates bacterial community assembly processes. The ISME Journal 15, 1943–1955.

Zhang, Y.Q., Li, W.J., Zhang, K.Y., Tian, X.P., Jiang, Y., Xu, L.H., Jiang, C.L., Lai, R., 2006. *Massilia dura* sp. nov., *Massilia albidiflava* sp. nov., *Massilia plicata* sp. nov. and *Massilia lutea* sp. nov., isolated from soils in China. International Journal of Systematic and Evolutionary Microbiology 56, 459–463.

Zhu, T., Zhang, J., Meng, T., Zhang, Y., Yang, J., Mueller, C., Cai, Z., 2014. Tea plantation destroys soil retention of NO_3^- and increases N_2O emissions in subtropical China. Soil Biology and Biochemistry 73, 106–114.

Zu, D., Wanner, G., Overmann, J., 2008. *Massilia brevitalea* sp. nov., a novel betaproteobacterium isolated from lysimeter soil. International Journal of Systematic and Evolutionary Microbiology 58, 1245–1251.